SMART ANTENNAS IN DIRECTION FINDING

Abstract. A smart antenna (or cognitive antenna or adaptive array) is a self-optimizing intelligent and interactive antenna which can help in the detection of the signal in case of background noise or interference. The work includes in designing the Smart Antenna as a transmitter of Uniform Rectangular Array (URA) of Reflector Backed Dipole Antenna (RBDA) placed at Netaji Subhash University of Technology (NSUT), East campus, New Delhi. The array is placed at a height of 169 meters above ground level. Each of the RBDA is operating at 10 GHz frequency. Five receiver locations are selected such that the antenna changes its beam pattern in order to find the maximum receiver placed in the nearby locations using amplitude scanning and steering vector techniques. The results concluded that when Taylor window is used for tapering the beam, the convergence of the algorithm is optimum.

Keywords: Taylor Window, Kaiser Window, Uniform Rectangular Array, Reflector Backed Dipole Antenna

I. INTRODUCTION

With the technological advancement, the use of smart antennas in future wireless system can help in efficient spectrum usage, minimizing new wireless networks, guranteed Quality of Service (QoS) and so on [1]. The major advantage of Smart Antenna Array includes in providing the narrowbeam towards the user of interest while nulling the other users which are part of the network [2]. This allow high signal-to-noise ratio with lower power in each cell (or Space Time Division Multiplexing). The another advantage of using the smart antennas include in the mitigation of the deleterious effect of multipath [3]. For the same, the constant modulus algorithm can be used in mitigating the multipath effect. This will help in reducing the receiver fading and high data rates can be achieved easily by reducing both the co-channel interference and multipath fading. These antenna can also be used in finding the direction (DF) more accurately by finding angle of arrival (AOA) [4]. The technique can be used in the radar system for accurately tracking the object. Some other advantages of using the Smart Antennas are Clutter Suppression, Blind Adaption, Multipath Mitigation, Space Divison Multiple Access (SDMA), improved system capabilities, higher signal to noise ratios, increased frequency reuse, sidelobe cancellation or null steering, MIMO capability in communication and radar systems [5].

Beam scanning is a technque to associate the main beam of the antenna array in the desired direction with the associated feed network [6]. There are two conventional techniques available for the beam scanning in phase array. The beam scanning can be achieved by either making variations in the phases of elements excitation or by frequency scanning. But both the techniques carry some disadvantages. The authors in [7] achieved the beam scanning by variation in magnitude of elements excitation. The beam scanning in phased arrays requires the linear phase distribution variation across antenna elements. This is accomplished either by using the variable phase shifters. The authors in [8] considered reflector backed antenna with loop-shaped parasitic elements to investigate the characteristics of S_{11} . It is found that the loop peripheral length and low-frequency resonance affects the dipole elements and length. Additionally, the high-frequency resonance gets affected by the peripheral length or the width perpendicular to the dipole. Neto et al, [9] illustrate that for scan of wide angles (45°), the connected arrays of dipole are the most suitable, that helps to retain the optimised number of receive or transmit modules. The wide band

matching can be obtained by the tuning of the reactive energy presented in the feeds of the connected dipoles. It gave 40% BW even at the scanning angle of 45° in case of lowest cross polarization level with a planer connected arrays of dipoles. With the growing research in the field of Machine Learning, the use of Artificial Neural Network (ANN) in the designing of smart antennas is emerging as the ANN can create the complex non-linear boundaries for classification purpose. Also, Neural Networks plays a predominant role in modelling the input output relation where the relation is quiet complex. Thus, Radial basis function (RBF), Multi-layer perceptron (MLP) and Hopefield Neural Network (HNN) are the most suitable Neural Network based technique for designing of smart antenna arrays [2].

This research will provide the amplitude based beam scanning technque to find the maximum coverage of the receiving antenna. To taper (apply weights) the beam, several windows are applied in order to get the maximum coverage of the receiver site. These include Taylor window, Tukey window, Blackman window, Chebyshev window and Kaiser window. The organization of the paper is as follows, section II will provide a basic comparsion between the smart and the traditional antenna. Section III will provide Reflector Backed Dipole Antenna with the *E* and *H* plane radiation pattern. Section IV will provide the windowing technques used to find the amplitude of the beam. Section V will provide the Direction Finding and Vector Steering techniques. Section VI will provide the results obtained while section VII will provide the conclusion and future scope of the work.

II. COMPARISON BETWEEN SMART ANTENNA ARRAY AND TRADITIONAL ARRAY

The traditional antenna arrays are fixed beam dumbed antenna array which doesnot change their radiation pattern according to the environment. These array doesnot posses any self healing power and the complete system needs to be changed once damaged or destroyed [10]. Since, the process of adaptive beam forming is not there in traditional antenna, hence the signal to noise ratio remain unaltered. Therefore, the radiation pattern obtained is unchanged as no algorithm is used for matching the output with the desired signal response. The smart antennas are the intelligent antenna patterns which adapt to change their beam pattern in accordance with the environment. They possess the self healing power when damaged and also posses low performance loss in case of any destroy [11]. These antennas adapt or adjust their beampatterns in such a way that maximum of the signal power is obtained while minimizing the noise content in the signal. There have been numerous of algorithms that have been developed for adaptive beamforming. These algorithms adjust the weight in such a way that the output matches with the desired signal response and the radiation pattern obtained is optimum radiation pattern.

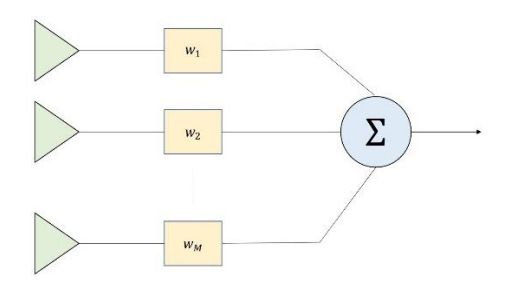
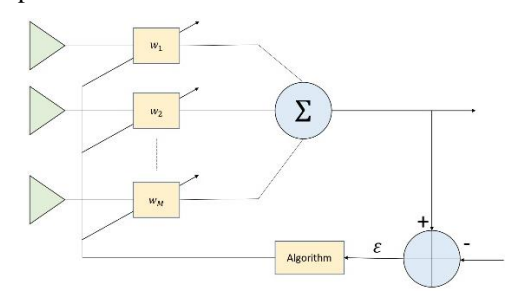


Figure 1: a) Showing the Traditional Antenna Array



b) Showing the Adaptive Beam forming pattern

III. REFLECTOR BACKED DIPOLE ANTENNA (RBDA)

A reflector antenna is a device used to reflect the electromagnetic waves in a specified direction. The antenna can take many form (geometries) but the most common includes in Plane, Corner and the Curved Reflector. For our analysis purpose, we use a simple Reflector Backed Dipole antenna with E-plane (x - z plane) radiation patterns in the far-field region [12] as

$$E_{\theta} = \sin(kH\cos\theta) \frac{\cos(kl_e\sin\theta) - \cos(kl_e)}{\cos\theta}$$
$$E_{\theta} = 0$$

while the H-plane (y - z plane) radiation patterns in the far-field region

$$E_{\theta} = 0$$

$$E_{\varphi} = \sin(kH\cos\theta)\cos(kw_e\sin\theta)$$

The directivity of RBDA is given by

$$G = \frac{4\pi}{\theta_{3E}\theta_{3H}}$$

and the achievable Electric field strength is given by

$$E = \frac{\sqrt{30P_TG}}{d} = \frac{\sqrt{120\pi P_T}}{d\sqrt{\theta_{3E}\theta_{3H}}}$$

where θ_{3E} and θ_{3H} are the 3 dB beamwidths of the test antenna in E plane and H plane respectively, while l_e and w_e represents the equivalent length and width respectively and P_T represents the radiated power of the test antenna.

IV. WINDOWING TECHNIQUES FOR TAPERING

Windows represent the finite duration sequences which are used to modify the impulse response of the FIR filter in order to provide smooth transition from pass band to stop band while reducing the ripples. In our work, different windows are used to adjust the weights of the beam scanner in order to receive the maximum coverage. The windows used in the study includes:

1. Dolph-Chebyshev Window: For a given Peak Side lobe level, this window achieves the narrowest mainlobe. The taper (weight) function of this window is defined by its frequency response and given as

$$W(f) = \frac{\Psi(f,N)\cos(\pi\sqrt{f^2-A^2})}{\cos(\pi\sqrt{-A^2})}$$
 where $A = \frac{\mathrm{acosh}(\eta)}{\pi} = \frac{\ln(\eta+\sqrt{\eta^2-1})}{\pi}$, $\Psi(f,N) = \begin{cases} +1, \ for \ N \ odd \ or \ f \geq 0 \\ -1, else \end{cases}$ and $\eta = 10^{-\frac{S}{20}}$ and S represents the side lobe level with respect to main lobe peak.

2. Taylor Window: This window approximates the Dolph-Chebyshev window's constant sidelobe level for a parametrized number of near-in sidelobes [13] and after that it allows the weight beyond this. This makes the window practically realizable and makes it popular for signal processing algorithms. The window function is given

$$w(t) = \left[1 + 2\sum_{m=1}^{(\bar{n}-1)} F_m \cos(2\pi mt)\right] \operatorname{rect}(t)$$

where the coefficients are calculated as

$$F_{m} = \frac{-\left[\frac{(-1)^{m}}{2}\right] \prod_{n=1}^{(\bar{n}-1)} \left[1 - \frac{\frac{m^{2}}{\sigma^{2}}}{A^{2} + \left[n - \frac{1}{2}\right]^{2}}\right]}{\prod_{n=1}^{(\bar{n}-1)} \left[1 - \frac{m^{2}}{n^{2}}\right]}, \text{ for } 1 \leq m \leq (\bar{n} - 1)$$

 $F_m = \frac{-\left[\frac{(-1)^m}{2}\right] \prod_{n=1}^{(\overline{n}-1)} \left[1 - \frac{\frac{m^2}{\sigma^2}}{A^2 + \left[n - \frac{1}{2}\right]^2}\right]}{\prod_{n=1}^{(\overline{n}-1)} \left[1 - \frac{m^2}{n^2}\right]}, \text{ for } 1 \leq m \leq (\overline{n}-1)$ with $\sigma^2 = \frac{(\overline{n})^2}{A^2 + \left(\overline{n} - \frac{1}{2}\right)^2}$ and $A = \frac{\operatorname{acosh}(\eta)}{\pi} = \frac{\ln(\eta + \sqrt{\eta^2 - 1})}{\pi}, \ \eta = 10^{-\frac{S}{20}}$ where \overline{n} represents the distance from the

mainlobe for which the sidelobes are constant. The Fourier transform of the continuous time window taper function is calculated to be

$$W(f) = \text{sinc}(f) + \sum_{m=1}^{(\bar{n}-1)} F_m(\text{sinc}(f-m) + \text{sinc}(f+m))$$

3. Tukey Window: This window is named after the American mathematician John Wilder Tukey. This window contains flat center while the edges contain cosine tapers [13]. It is also a parametric window, and the function is given as

$$w(x) = \begin{cases} \frac{1}{2} \left\{ 1 + \cos\left(\frac{2\pi}{r} \left[x - \frac{r}{2}\right]\right) \right\}, & 0 \le x < \frac{r}{2} \\ 1, & \frac{r}{2} \le x < 1 - \frac{r}{2} \\ \frac{1}{2} \left\{ 1 + \cos\left(\frac{2\pi}{r} \left[x - 1 + \frac{r}{2}\right]\right) \right\}, & 1 - \frac{r}{2} \le x \le 1 \end{cases}$$

The parameter r is defined by the ratio of cosine-tapered section to the entire window length and ranges from $0 \le r \le 1$.

4. *Kaiser Window:* The approximation of ideal Maximum Energy taper is given by this equation. In the ideal Maximum Energy taper, the calculation of prolate spheroidal wave function is difficult and therefore, the scientist approximates the calculation based on zero-order modified Bessel function [13]. The coefficient of kaiser window can be calculated using the following equation as

$$w(n) = \frac{I_0 \left(\beta \sqrt{1 - \left(\frac{n - \frac{N}{2}}{\frac{N}{2}}\right)^2}\right)}{I_0(\beta)}, 0 \le n \le N$$

where I_0 represents the zeroth-order modified Bessel function of first kind and

$$\beta = \begin{cases} 0.1102(\alpha - 8.7), & \alpha > 50\\ 0.5842(\alpha - 21)^{0.4} + 0.07886(\alpha - 21), & 50 \ge \alpha \ge 21\\ 0, & \alpha < 21 \end{cases}$$

5. **Blackman Window**: The blackman window is an extension of the Generalized Raised Cosine window where the window adds another cosine term to the existing constant and single cosine term [13]. The addition of extra cosine term helps in the optimization of window taper function spectral characteristics. The general equation for blackman window is given as

$$w(n) = 0.42 - 0.5\cos\left(\frac{2\pi n}{L-1}\right) + 0.08\cos\left(\frac{4\pi n}{L-1}\right)$$

V. DIRECTION FINDING and VECTOR STEERING

The direction is found using the Angle-of-Arrival approach. The directional finding algorithms not only rely on received signal strength (RSSI) but also depends upon actual direction of the signal which makes the positioning easier. For finding the direction, we considered Amplitude Scanning Technique given by [7]. The array uses only one fixed phase shifters and two amplitude control or signal splitters. Hence, the array factor is given by

$$\mathrm{AF} = \sum_{n=1}^N e^{j(n-1)(kd\cos\theta + \beta)}.$$

Much of the research work is done on direction finding and beamforming using the scalar sensor array. These are capable of extracting only one component from the electric or magnetic field for processing. The angle of arrival estimation with proper accuracy requires complete vector field of polarization called vector sensor. The ideal vertical electric dipole can only detect Vertical Electric Field while the ideal horizontal dipole can only respond to Vertical Magnetic Field. The cross product of Electric and Magnetic field is given by poynting vector $(\overline{S} = \overline{E} \times \overline{H})$ which indicates the propogation of the direction of the incident wave and can be converted to Angle-of-Arrival estimation. Hence by replacing the scalar antennas with the vector sensor antennas, the angle of arrival can be estimated by both the approaches which include cross-product direction finding technique and traditional direction finding technique.

Steering Vector is the parametric representation of the vector sensor response to a uniform plane wave signal originating from any angle of arrival. CART is the traditional physical confriguation for the vector sensor processing and composed of 3-electric dipole antennas and 3-loop antennas or magnetic dipoles. The Electric dipole antennas are used to measure the Electric field components E_x , E_y , E_z while the Loop antenna are used to measure Magnetic field components H_x , H_y , H_z of the transverse electromagetic wave (TEM). The CART vector sensor is sensitive to

two-dimensions that includes angle-of-arrival and polarization of the incident plane wave. The vector sensor steering can be expressed in terms of angle of arrival (θ, Φ) and polarization state (Υ, η) of the incident plane wave of individual Electric and Magnetic field components for all the six axes E_x , E_y , E_z , H_y , H_y , H_z .

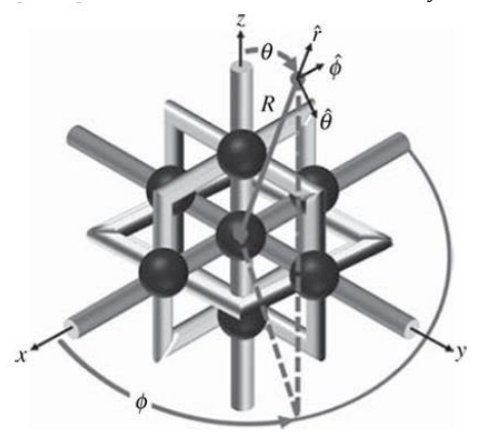


Figure 2: CART Vector sensor antenna and coordinate system definition

The general form of vector sensor steering vector is given by

$$\bar{a}(\theta, \Phi, Y, \eta) = \begin{bmatrix} E_x \\ E_y \\ E_z \\ H_x \\ H_y \\ H_z \end{bmatrix} = \begin{bmatrix} \cos\theta\cos\phi & -\sin\phi \\ \cos\theta\sin\phi & \cos\phi \\ -\sin\theta & 0 \\ -\sin\phi & -\cos\theta\cos\phi \\ \cos\phi & -\cos\theta\sin\phi \\ 0 & \sin\theta \end{bmatrix} \begin{bmatrix} \sin(Y) e^{j\eta} \\ \cos(Y) \end{bmatrix} = \bar{\Theta}(\theta, \Phi)\bar{p}(Y, \eta)$$

The few observations about the vector sensor steering includes first the steering vector size of 6×1 means that single six-axis vector sensor contains six, scalar antenna that are co-located and are co-centered at a single location. The advantage of co-location and co-centre includes in the induction of no time delay between the elements. Second, the steering vector is also sensitive to the polarization of state and hence it is practically possible to separate the signals which arrive from the same direction. Third, it is also possible to separate the estimation of the angle of arrival from the polarization state which helps in simplifying the Direction-Finding Algorithms.

For our application, M signals arrive with the unique arrival angles and polarization states $\overline{\psi_m} = (\theta_m, \Phi_m, \gamma_m, \eta_m)$ such that the instantaneous response of the single vector will be given by where w and Φ are the carrier frequency and the phase of the incoming signal s(t)

$$\overline{x_m}(t) = \overline{g}(\theta_m, \Phi_m) \overline{a}(\theta_m, \Phi_m, \gamma_m, \eta_m) E_{o,m} e^{j(w_m t + \Phi_m)} + \overline{n}(t)$$

$$s(t) = E_o e^{j(wt + \Phi)}$$

and $\bar{n}(t)$ is a 6×1 additive complex valued noise vector. Hence the steering vector for the l^{th} vector sensor due to m^{th} signal is given by and thus the response due to l^{th} vector sensor

$$\overline{v_{vs,l}}(\overline{\psi_m}) = q_l(\theta_m, \Phi_m) \overline{a}(\overline{\psi_m}) = q_l(\theta_m, \Phi_m) \overline{\theta}(\theta_m, \Phi_m) \overline{p}(\Upsilon_m, \eta_m)$$

in the array is generated by concatenating the L steering vectors which is finally given by

$$\overline{v_{vs}}(\overline{\psi_m}) = \begin{bmatrix} \overline{v_{vs,1}}(\overline{\psi_m}) \\ \vdots \\ \overline{v_{vs,L}}(\overline{\psi_m}) \end{bmatrix}$$

with complete normalized response $\overline{x_m}(t) = \overline{v_{vs}}(\overline{\psi_m})s_m(t) + \overline{N}(t)$.

VI. RESULTS

We consider a 7 × 7 Uniform Rectangular Array of RBDA as shown in figure 3b. Each of the reflector dipole antennas is operating at 10 GHz frequency and radiating in xy plane. The spacing between each element is $\frac{\lambda}{2}$ and the array is placed in yz-plane with the radiation in the x-direction. The radiation pattern for all the combined antennas is shown in figure 3c. We create a transmitter site at our college NSUT East campus with the corresponding latitude (28.654470) and longitude (77.268027) using the antenna array formed above shown in figure 3b. The frequency of the transmitter should be matched with the antenna's design frequency in order to get the maximum power. The

transmitted output power is set to 1 W with the antenna height of 169 meters. Hence, figure 4a shows the image of the transmitter situated at **campus** from the US Geographical survey map while figure 4b shows the corresponding radiation pattern.

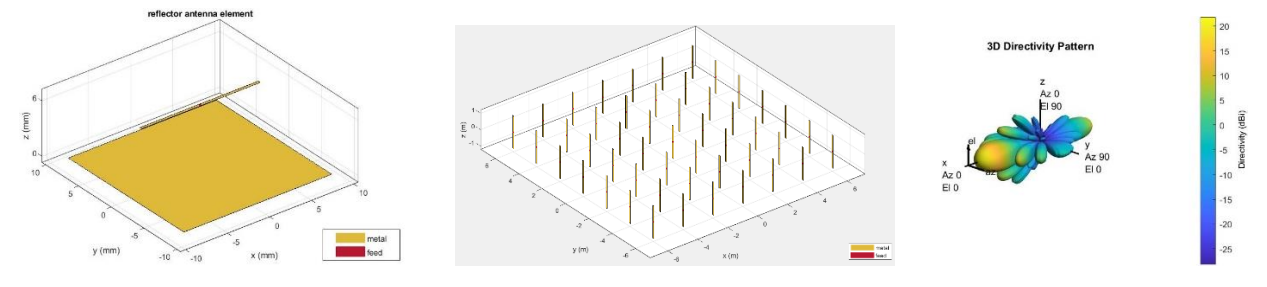


Figure 3: a) Reflector Backed Dipole Antenna b) Showing 7×7 Uniform Rectangular Array of Reflector Backed Dipole Antenna c) Showing the radiation pattern from all the array elements

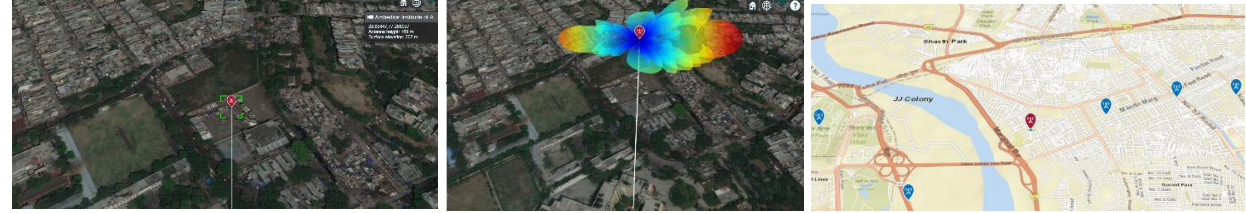
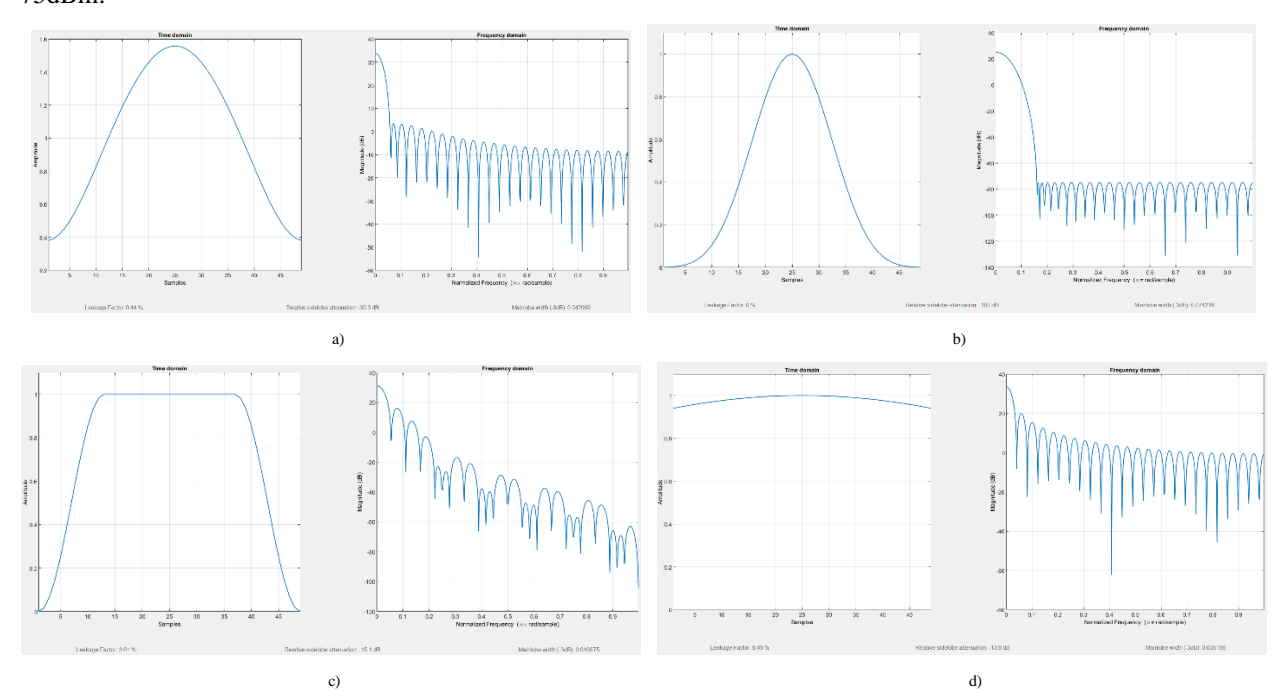


Figure 4: a) Showing the transmitter placed at Ambedkar Institute with height 169 meters b) Showing the radiation pattern at transmitter site c) Showing the receiver site location

An array of five receiver sites is considered using the latitude and longitude of the sites taken from Google Map as shown in figure 4c. These are the sites of interest which possess the access of the coverage from the transmitter site. These five sites include monument, hospital, temple, marketplace and college area to visualize the application of Smart Antenna. The names for these sites include *Red Fort, Shri Ram Singh Hospital, Raghunath Temple, Pusta bazar* and *Northern India regional council of ICAI*. The corresponding latitude and longitude of the receiver sites include (28.656311, 77.241079) of Red Fort, (28.660581, 77.287640) of Shri Ram Singh Hospital, (28.657961, 77.277826) of Raghunath Temple, (28.647140, 77.254341) of Pusta Bazar and (28.660942, 77.295757) of Northern India regional council of ICAI. The array of all receiver sites is formed with each receiver having a sensitivity of -75dBm.



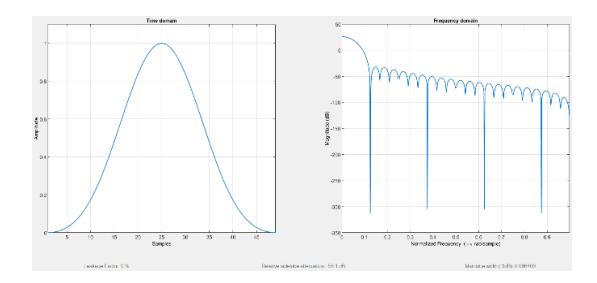


Figure 5: Showing the Time and Frequency domain representation of a) Taylor Window b) Chebyshev Window c) Tukey Window d) Kaiser Window e) Blackman Window

The beam is scanned by applying the taper for a range of angles. For each angle, the antenna updates its radiation pattern over a sweep angle of -20° to 20° . The windowing techniques are used for tapering the beam with the given sweep angle. Figure 5 includes the time and frequency domain representation for all the above-mentioned windows. Finally, we update the radiation pattern of the transmitter using the weights assigned by each of the windowing technique. This approach of beam produces different radiation patterns then the physically rotating antenna. We also define the three signal strength levels in red, yellow and green color as shown in figure 6a. The red color shows the maximum signal strength while the yellow color shows medium signal strength, and the green color shows weak signal strength. The received power includes the total transmitted power from the Uniform Rectangular Array. Hence, we finally display the coverage map out to 6000 meters or 6 kilometers. The results show that there is no coverage on the transmitter site and there are a couple of coverages along the bore sight direction. The radiation pattern provides us an understanding of how the antenna power projects onto the map locations around the transmitter. Figure 6 will depict the power corresponding to each receiver site with the maximum coverage area of the transmitter site. Once, we receive the coverage area our target is to map maximum receiver sites in the same coverage area only for which we apply the same algorithm (taper for range of angles) discussed above with the steering vector. The algorithm will work number of times unless the transmitter gets the maximum receivers in their coverage area site. This will assign a sweep of angles taper from the steering vector. Once the transmitter gets maximum receiver in the coverage area, the algorithm will automatically be stopped, and the intermediate and final images are shown. Hence, we develop the concept of adaptive beams forming with the help of the transmitter from the above. The similar concept can be placed in the radar system to detect the target by sweeping for a range of angles. It is not always mandatory that the pulse send over the target should include the target in the very first time. Hence, the radar system first identifies the target by scanning over a beam for many sweep angles and then only the range can be estimated.



Figure 6: a) Showing the radiation pattern of the transmitter with respect to the receiver site b) Showing the last sweep of the beam by the transmitter to finally detect our receiver site

For calculating the complexity of different windowing techniques, we plot a bar graph as shown in figure 7. From the graph, Taylor window converges at much faster rate than the other windowing techniques used for tapering the beam while the Blackman window converges the least amongst all. This is because of the sidelobe cancellation property.

VII. CONCLUSION and FUTURE WORK

We have designed a URA of RBDA antenna. We analyze the radiation pattern and apply different windowing techniques in order to get the weights for the beam and made a sweep in order to find the maximum coverage.

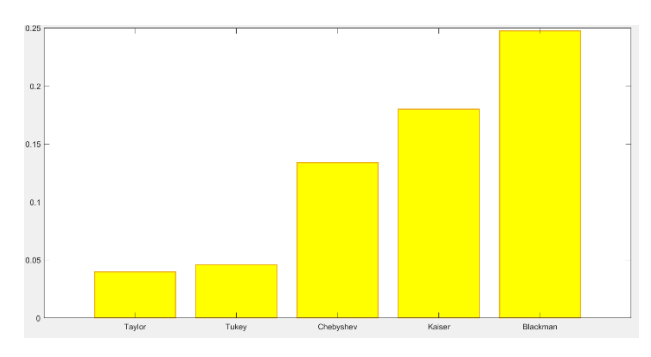


Figure 7: Showing the Time Complexity of different windowing technique

The scope future of the work will be in the analysis of Smart Antenna using other more robust adaptive signal processing algorithms and to apply beamforming algorithms instead of beam scanning techniques.

VII. REFERENCES

- 1. Alexiou, A. and Haardt, M., 2004. Smart antenna technologies for future wireless systems: trends and challenges. *IEEE communications Magazine*, 42(9), pp.90-97.
- 2. Rawat, A., Yadav, R.N. and Shrivastava, S.C., 2012. Neural network applications in smart antenna arrays: A review. *AEU-International Journal of Electronics and Communications*, 66(11), pp.903-912.
- 3. Abdala, M.A. and Al-Zuhairy, A.K., 2013. Integration of Smart Antenna System in Mobile Ad Hoc Networks. *International Journal of Machine Learning and Computing*, *3*(4), pp.342-346.
- 4. Sharma, B., IndranilSarkar, T.M. and Bhattacharya, P.P., 2014. An introduction to smart antenna system. *International Journal of Business and Engineering Research*, 8, pp.22-26.
- 5. Balanis, C.A. and Ioannides, P.I., 2007. Introduction to smart antennas. *Synthesis Lectures on Antennas*, 2(1), pp.1-175.
- 6. Liao, P. and York, R.A., 1993. A new phase-shifterless beam-scanning technique using arrays of coupled oscillators. *IEEE transactions on microwave theory and techniques*, 41(10), pp.1810-1815.
- 7. Sayidmarie, K.H. and Saghurchy, M.N., 2011, November. Array beam scanning by variation of elements amplitude-only excitations. In 2011 4th IEEE International Symposium on Microwave, Antenna, Propagation and EMC Technologies for Wireless Communications (pp. 749-753). IEEE.
- 8. Sasaki, T., Cho, K., Ihara, T. and Yoshihara, T., 2014, August. Influence of loop parasitic elements on bandwidth improvement of reflector backed Dipole antenna. In 2014 IEEE International Workshop on Electromagnetics (iWEM) (pp. 56-57). IEEE.
- 9. Neto, A., Cavallo, D., Gerini, G. and Toso, G., 2009. Scanning performances of wideband connected arrays in the presence of a backing reflector. *IEEE Transactions on Antennas and Propagation*, 57(10), pp.3092-3102.
- 10. Lu, J., Schlub, R. and Ohira, T., 2001, December. A performance comparison of smart antenna technology for wireless mobile computing terminals. In *APMC 2001. 2001 Asia-Pacific Microwave Conference (Cat. No. 01TH8577)* (Vol. 2, pp. 581-584). IEEE.
- 11. Ertel, R.B., Cardieri, P., Sowerby, K.W., Rappaport, T.S. and Reed, J.H., 1998. Overview of spatial channel models for antenna array communication systems. *IEEE personal communications*, 5(1), pp.10-22.
- 12. Wu, Q. and Su, D., 2013. On the broadband reflector-backed dipole antennas with wide beamwidth for the EMC tests of large equipment above 1 GHz. *IEEE transactions on electromagnetic compatibility*, 55(6), pp.999-1006.
- 13. Doerry, A.W., 2017. *Catalog of window taper functions for sidelobe control* (No. SAND2017-4042). Sandia National Lab.(SNL-NM), Albuquerque, NM (United States).